Acknowledgements

We are grateful to L. Ottolini for SIMS facilities at CSCC, Pavia. The financial support of the CNR "Centro di Studio per la Geodinamica Alpina" (Padova) and of MURST grants is gratefully acknowledged.

References

Burt, M.D. (1980) The stability of danalite, $Fe_4Be_3(SiO_4)_3S$. *Amer. Mineral.*, **65**, 355–60.

Hassan, I., and Grundy, H.D. (1985) The crystal structures of helvite group minerals, $(Mn,Fe,Zn)_8(Be_6Si_6O_{24})S_2$. *Amer. Mineral.*, **70**, 186–92.

Holloway, W.M. Jr., Giordan, T.J. and Peacor, D.R. (1972) Refinement of the crystal structure of helvite, $Mn_4(BeSiO_4)_3S$. *Acta Crystallogr.*, **B28**, 114–7.

International Tables for X-ray Crystallography (1974) J.A. Ibers and W.C. Hamilton (Eds.), vol. 4, pp. 99–101, Kynoch Press, Birmingham.

Ishihara, S. (1977) The magnetite-series and ilmenite-series granitic rocks. *Mining Geol.*, **27**, 293–305.

Kwak, T.A.P. and Jackson, P.G. (1986) The compositional variation and genesis of danalite in Sn-F-W skarns, NW Tasmania, Australia. *Neues Jahrb. Mineral., Mh.*, 452–62.

Larsen, A.O. (1988) Helvite group minerals from syenite pegmatites in the Oslo Region, Norway. Contribution to the mineralogy of Norway, No 68. *Norsk. Geol. Tidsskrift*, **68**, 119–24.

Mel'nikov, O.K., Litvin, B.M. and Fedosova, S.P. (1968) Production of helvite-group compounds [in Russian]. In: *Gidrotermal'nyi Sintez Kristallov*, (A.M. Lobachev, ed.). pp. 167–74, Nauka Press, Moscow (quoted in Burt, 1980).

Ottolini, L., Bottazzi, P. and Vannucci, R. (1993) Quantification of lithium, beryllium, and boron in silicates by Secondary Ion Mass Spectrometry using conventional energy filtering. *Anal. Chem.*, **65**, 1960–8.

Pauling, L. (1930) The structure of sodalite and helvite. *Zeit Krist.*, **74**, 213–25.

Ragu, A. (1994) Helvite from the French Pyrénées as evidence for granite-related hydrothermal activity. *Can. Mineral.*, **32**, 111–20.

Shannon, R.D. (1976) Revised effective ionic radii and systematic studies of interatomic distances in halides and chalcogenides. *Acta Crystallogr.*, **A32**, 251–5.

Tokonami, M. (1965) Atomic scattering factors for O^{2-}. *Acta Crystallogr.*, **16**, 486.

Visonà, D. (1993) The Daba Shabeli gabbro-syenite complex: an element of the gabbro belt in the Northern Somali basement. In: *Geology and mineral resources of Somalia and surrounding regions.* (E. Abbate, M. Sagri and F.P. Sassi, eds.) *Bull. Ist. Agronom. Oltremare*, special issue, **113 A**, 59–82, Firenze.

Zachariasen, W.H. (1963) The secondary extinction correction. *Acta Crystallogr.*, **16**, 1139–44.

[*Manuscript received 20 September 1994: revised 6 April 1995*]

KEYWORDS: danalite, Daba Shabeli Complex, Somalia, crystal chemistry

MINERALOGICAL MAGAZINE, APRIL, VOL. 60, PP 379–387

Subsilicic sodium gedrite in leptite of quartz keratophyric origin, Nordmark (Sweden)

Kees Linthout
Wim J. Lustenhouwer

Institute of Earth Sciences,
Vrije Universiteit,
De Boelelaan 1085,
1081 HV Amsterdam,
The Netherlands

THE Mg–Fe orthoamphibole series $\square(Mg,Fe)_7Si_8O_{22}(OH)_2$–$Na(Mg,Fe)_5Al_2Si_5Al_3O_{22}(OH)_2$ has an open end in the sense that the Si_5 end member has not been found in nature; tiny domains of near end-member composition in intricately zoned crystals (Schumacher, 1980;

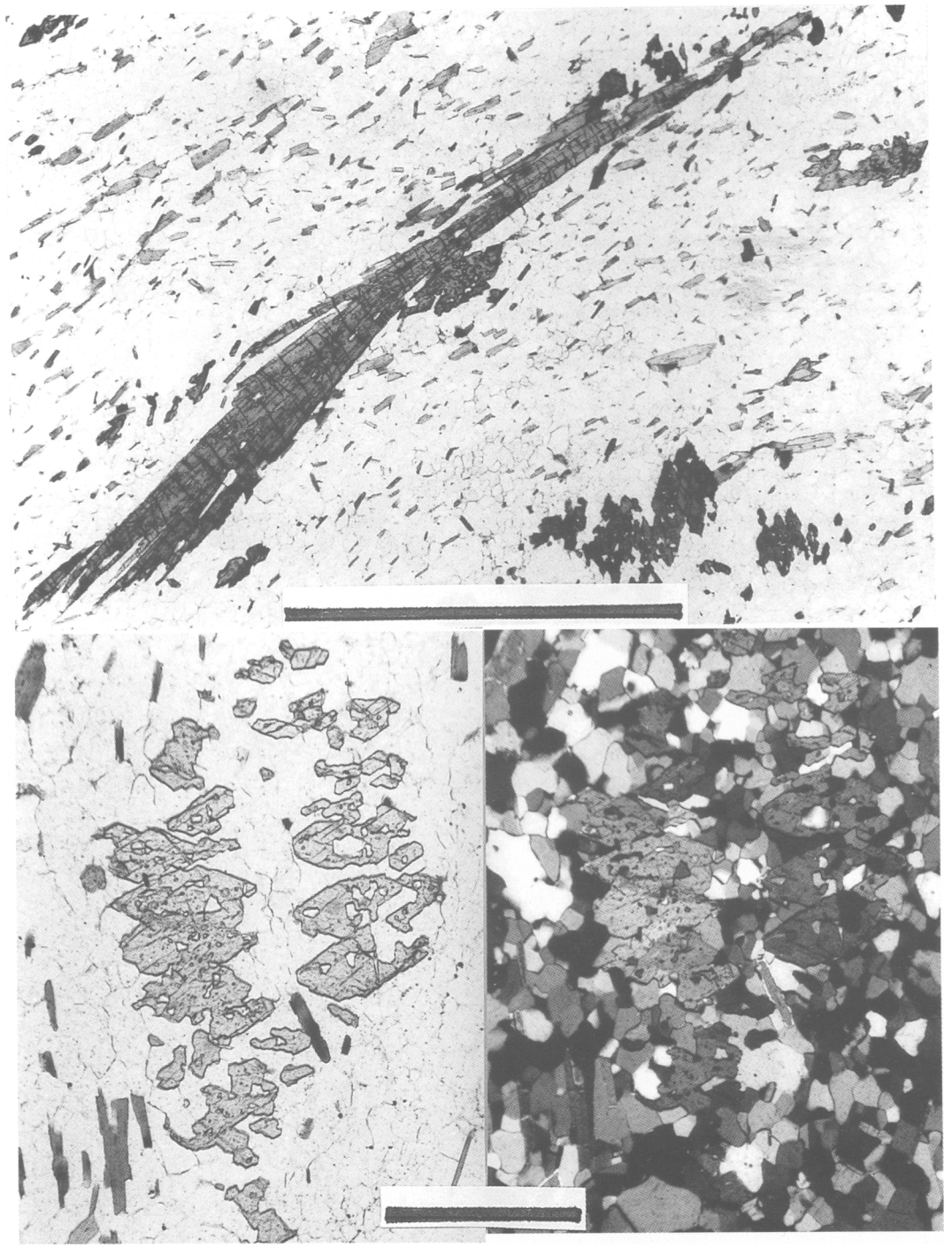

FIG. 1. Microphotographs, in plane polarized light (a,b) and between crossed polarizers (c), showing sheaf-like bundle and {210} cross sections of subsilicic sodium gedrite, set in a very fine-grained polygonal quartz-albite matrix, also containing fine-grained biotite flakes. Scale bars are 1 mm.

Robinson *et al.*, 1982), appeared to be intergrowths of two different double-chain silicates (Schumacher, pers. comm., 1994).

This is a first account of clear and distinct (4 mm) crystals of largely subsilicic sodium gedrite, i.e. with $Na^A \geqslant 0.5$ and $Si < 5.75$ (IMA nomenclature; Leake, 1978). The optical properties and cell dimensions for this extreme corner in the amphibole compositional space have not been reported before. Crystal chemistry, substitution patterns and paragenesis of (subsilicic) gedrites are discussed.

[Subsilic sodium gedrites from the literature are poorly crystallized (<300 μm), intergrown either with sillimanite and quartz vermiforms (Kroonenberg, 1976), or with andalusite and sekaninaite (Damman, 1988), and their optical or X-ray data were not given.]

Petrological setting

The subsilicic sodium gedrite occurs in felsic metavolcanics (leptites) in Nordmark, central Sweden (mapsheet 11E Filipstad NV, 6640.00/1403.42). Wide-spread andalusite and cordierite in metasediments (Magnusson, 1970), preserving detailed (microscopic) sedimentary textures (Roep and Linthout, 1990), indicate the prevalence of medium-grade, static, low-pressure metamorphism in the Nordmark area.

Set in a very fine-grained (0.05 mm) polygonal quartz-albite matrix, subsilicic sodium gedrite forms up to 4 mm large sheaf-like bundles of euhedral {210} prisms (Fig. 1), locally concentrated in sub-parallel patches and streaks. Quartz and albite further occur as mm-sized pseudomorphs after phenocrysts of HT quartz and feldspar. The albite phenocrysts, for one part twinned according to the Carlsbad-albite law and for another showing the 'chessboard' pattern, are interpreted as albitized plagioclase and K-feldspar, respectively. Greenish brown flakes (0.4 mm) of biotite occur intergrown with the amphibole as well as dispersed in the matrix. Subordinate ilmenite forms platelets ($\leqslant$0.1 mm). Chlorite aggregates have partly replaced biotite and amphibole. Euhedral blasts of chloritoid and staurolite formed inside these aggregates during a later stage of intermediate-pressure metamorphism (Linthout, 1983*a*), and thus are not cogenetic with the amphibole.

Abundance of phenocrystic quartz in the SiO_2-rich leptite suggests a rhyolitic origin. However, the rock's CaO and K_2O contents are significantly below the averages given for pristine rhyolites, and the FeO and MgO contents are relatively high (Table 1). Considering that synvolcanic sub-seafloor hydrothermal alterations are wide-spread in the supracrustals of western Bergslagen (Baker and De Groot, 1983, Lagerblad and Gorbatschev, 1985), the protolith of the host rock can be qualified as quartz keratophyre, a common rock-type in low-grade metamorphic areas of Bergslagen (Linthout, 1983*b*). *Mutatis mutandis,* the explanation is compatible with Vallance's (1967) generally accepted concept that many orthoamphibole–cordierite(/staurolite) rocks are amphibolite-facies spilites (see Spear, 1993, for a recent summary and references). The concept, however, does not apply to the other two occurrences of subsilicic sodium gedrite. Kroonenberg's (1976) 'ferrogedrite' occurs in a Ca-poor metapelitic gneiss (amphibolite facies, 680°C, 5–7 kbar), but only in sekaninaite-rich, K-deficient clots, created in a preceding stage of metamorphic/migmatitic differentiation in the granulite facies. Damman's (1988) subsilicic sodium gedrite formed with andalusite and sekaninaite in hydrothermal veins (560°C, 1 kbar).

Optical properties and cell dimensions

In Na-light, $n_\alpha = 1.683$, $n_\gamma = 1.700$, $2V_\alpha \approx 85°$, and $\Delta n = 0.0175$. Absorption $\gamma > \beta > \alpha$ is strong, with pale yellow $\parallel \alpha$, bluish grey $\parallel \beta$, and grey green $\parallel \gamma$. Halos around zircon inclusions are red-brown.

Cell dimensions computed from 24 reflections (Guinier powder-diffraction, Co-K_α) are given in Table 2. Indexing of most reflections, consistent with the space group *Pnma*, follows Seitsaari (1956) and Seki and Yamasaki (1957).

Plotting n_γ *vs. b* (Fabriës and Perseil, 1971) indicates iron-rich gedrite with $Al^{IV} > 2$ a.p.f.u..

The positive correlation, shown by the *a* values and Na a.p.f.u. of the Nordmark specimen and

TABLE 1. Compositions of leptite from Nordmark and average rhyolite after Le Maitre (1976)

	Leptite LT78B2	Average rhyolite
SiO_2	77.4	72.82
TiO_2	0.172	0.27
Al_2O_3	11.52	13.53
Fe_2O_3	–	1.48
FeO	3.87[t]	1.11
MnO	0.031	0.06
MgO	1.31	0.39
CaO	0.19	1.14
Na_2O	3.78	3.55
K_2O	0.808	4.30
P_2O_5	0.030	0.07
H_2O (+/–)	–	1.10/0.31
CO_2	–	0.08
total	99.11	99.96

t: all iron as FeO

TABLE 2. Cell dimensions and compositional data of subsilicic sodium gedrite from Nordmark (1) and gedrites *s.l.*, nearest in composition, with published X-ray data; (2) Papike and Ross (1970); (3) Seitsaari (1956); (4) Seki and Yamasaki (1957)

	1	2	3	4
a (Å)	18.620(6)	18.601(4)	18.596	18.514
b (Å)	17.878(6)	17.839(3)	17.899	17.945
c (Å)	5.304(2)	5.284(2)	5.295	5.316
V (Å^3)	1765.6(15)	1753.2(6)	1762.5	1766.0
Na	0.675	0.535	0.33	0.15
Al^{IV}	2.254	2.047	2.31	1.97
Al^{VI}	1.583	1.365	1.27	1.68
X_{Mg}	0.24	0.56	0.21	0.002

TABLE 3. Compositions of subsilicic sodium gedrite, biotite and albite from Nordmark (Sweden)

	Subsilicic sodium gedrite						Biotite	Albite
	average,	n=17 (range)	Na max.	Na min.	Fe max.	incl. F		
SiO_2	37.17	(36.71–37.85)	36.77	37.85	37.34	37.07	35.05	68.35
TiO_2	0.08	(0.04–0.16)	0.05	0.11	0.16	0.11	1.28	
Al_2O_3	21.06	(20.29–21.99)	21.99	20.41	20.29	21.33	17.90	18.84
FeO^t	30.69	(28.48–32.35)	29.62	31.29	32.35	32.14	24.04	
MnO	0.82	(0.57–0.99)	0.83	0.97	0.71	0.59	0.05	
MgO	5.68	(4.77–6.81)	6.62	5.38	5.01	4.77	7.55	
BaO	–	–	–	–	–	0.11		
CaO	0.08	(0.05–0.11)	0.07	0.08	0.07	0.09	n.d.	0.24
Na_2O	2.25	(2.00–2.51)	2.51	2.00	2.031	2.31	0.31	11.59
K_2O	n.d.		n.d.	n.d.	n.d.	n.d.	9.35	0.02
F	–		–	–	–	0.27	0.77	
Cl	–		–	–	–	n.d.	0.02	
H_2O (calc.)	1.94		1.96	1.94	1.93	1.81	3.49	
O ≡ F,Cl	–		–	–	–	–0.11	–0.33	
Total	99.77		100.42	100.03	99.89	100.38	99.59	99.04
Si	5.746		5.625	5.843	5.805	5.728	5.454	3.012
Al^{IV}	2.254		2.375	2.157	2.195	2.272	2.546	0.979
Al^{VI}	1.583		1.590	1.557	1.522	1.613	0.737	
Ti	0.009		0.006	0.013	0.019	0.013	0.150	
Fe^{2+}	3.968		3.790	4.040	4.205	4.153	3.128	
Mg	1.309		1.510	1.238	1.161	1.099	1.751	
Mn	0.107		0.108	0.127	0.093	0.077	0.007	
Ca	0.013		0.012	0.013	0.012	0.015	–	0.011
Na	0.674		0.745	0.598	0.612	0.692	0.094	0.991
K	–		–	–	–	–	1.856	0.001
Ba	–		–	–	–	–	0.007	
F	–		–	–	–	0.132	0.379	
Cl	–		–	–	–	–	0.005	
ΣT,M ex. Na	14.989		15.014	14.988	15.013	14.970		
X_{Mg}	0.24		0.28	0.23	0.21	0.21	0.36	
Na^A/Al^{IV}	0.30		0.31	0.28	0.28	0.30		

t: all iron as FeO; n.d.: none detected

gedrites nearest in composition (Table 2), cannot be attributed directly to an increase of the A-site filling, as anion–cation distances in the A-site of ortho-amphiboles get shorter with larger Na^A values (Hawthorne, 1983). More likely, the concomitant replacement of Si by Al^{IV} is causing the large *a* values. The high Al^{IV} content of the subsilicic sodium gedrite also contributes to the cell volume which is as large as that of a ferro-gedrite (Seki and Yamasaki, 1960), owing its large volume to a large *b* dimension, related to a low X_{Mg} (Popp *et al.*, 1976).

Chemical composition and unit formula

Electron microprobe analyses were carried out with a Cambridge Instruments Ltd. Microscan-9, with 15 kV acceleration voltage, 50 nA specimen current on a Faraday cup and 15 s counting time, except 50 s for F. Well-calibrated natural and synthetic standards were used. The analyses were ZAF corrected with the Microscan-9 on-line program. Considering the counting statistics and various corrections, the precision of the method is better than 1%. Totals of 17 amphibole analyses, inclusive of calculated H_2O, vary from 99.31 to 100.42 wt.%, which compares well with Leake's (1968) suggestion (for Ca amphiboles) that superior analyses should have totals of oxides within the range 99.40 to 100.60 wt.%. Measured in four sites, F amounts to about 0.26 wt.%. If present, K_2O and Cl are below 0.01 wt.%. Exsolution lamellae could not be detected with the electron microprobe. A weak preference of Si, Ti and Ca for the cores and of Al and Na for the rims, can be observed. A more pronounced variation in the inversely correlated Mg and Fe, however, appears not to be zonary. Table 3 gives, in addition to the average, three extreme compositions and one with analysed F.

Cations, calculated on the basis of O_{23}, assuming total iron as FeO, were assigned to structural positions following the IMA procedure (Leake, 1978). Sums of cations excluding Na^+ are close to 15 a.p.f.u., the ideal value for $\Sigma T,M$ in ortho-amphiboles (Hawthorne, 1983). Assuming either tiny quantities ($\leqslant$ 0.032 a.p.f.u.) of Na^{M4} or of less than 1.2% of total iron as Fe^{3+}, will force $\Sigma T,M$ to 15. Consequently, calculation of any Fe^{3+} is considered trivial.

The average composition lies in the heart of the end-member trilateral sodium gedrite, with $Na^A(Mg,Fe)_6Al^{VI}Si_6Al^V$, the not yet named MgFe-pendant of sadanagaite, with $Na^A(Mg,Fe)_5Al_2^{VI}Si_5Al_3^{IV}$, and gedrite, with $\square^A(Mg,Fe)_5Al_2^{VI}Si_6Al_2^{IV}$ (Fig. 2).

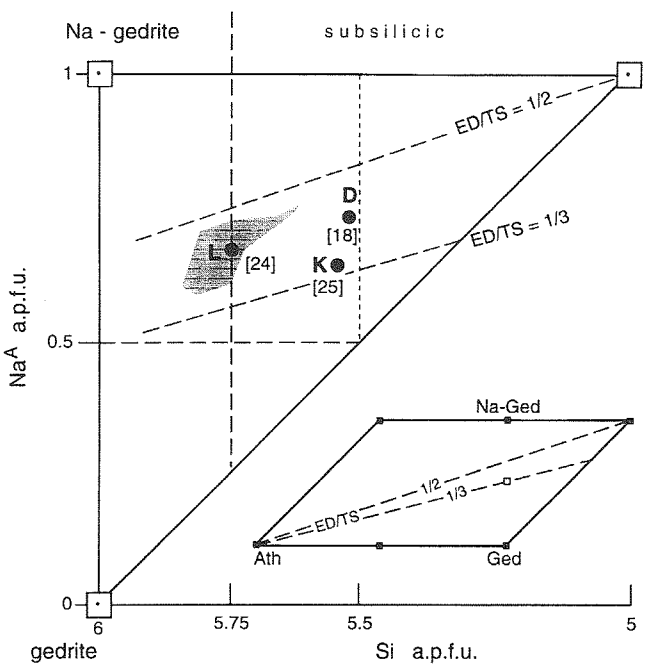

FIG. 2. Plot of Na^A *vs.* Si of subsilicic sodium gedrites. Shaded field with average L: Nordmark data; K: Surinam (Kroonenberg, 1976); D: Bergslagen (Damman, 1988). Mg/(Mg + Fe + Mn) as [%]. ED/TS is explained in text. Symbols for minerals after Kretz (1983). Open square in inset marks 'ideal gedrite' (see text).

Coupled substitutions in gedrites *s.l.*

Compositions of gedrites are often discussed in terms of X_{Mg} [= Mg/(Mg+Fe+Mn)] and the coupled substitutions $Na^{A}Al^{IV} = \square^{A}Si$ (edenitic, ED) and $Al^{VI}Al^{IV} = MgSi$ (tschermakitic, TS) by which their formulae can be derived from that of end-member anthophyllite (Robinson *et al.*, 1971). The ED/TS ratios for gedrites of many areas vary from 0.1 to unity (Berg, 1985). In the Nordmark sample ED/TS = 0.38–0.47, keeping the middle between the major trend ED/TS = 1 : 3 from anthophyllite through 'ideal gedrite' (with $Na^{A}_{0.5}Al^{VI}_{1.5}Al^{IV}_{2}$, once thought to be end member in this series, see Robinson *et al.*, 1971) and ED/TS = 1 : 2 towards the composition with maximum ED and TS substitutions (Fig. 2).

Compositional trends in suites of gedrites have been used to describe the supposed dependence of Na^{A}, Al^{VI} and Al^{IV} on X_{Mg} (Robinson *et al.*, 1971; Spear, 1980). A general inverse correlation between Na^{A}/Al^{IV} and X_{Mg}, seen by Berg (1985), was questioned by Damman (1988), who pointed at the wide spread of X_{Mg} (0.15–0.62) in a narrow range of Na^{A}/Al^{IV} (0.31–0.36). However, a second look at Berg's diagram, supplemented with data from iron-rich gedrites, reveals that, per metamorphic area, suites of gedrites with $X_{Mg} > 0.33$ do show the proposed inverse correlation; on the other hand, for suites of gedrites with $X_{Mg} < 0.33$ a positive correlation between Na^{A}/Al^{IV} and X_{Mg} is discernible (Fig. 3). Moreover, the Na^{A}/Al^{IV} peak at 0.5, as embodied in Berg's (1985) sodium gedrite, occurs at about $X_{Mg} = 0.33$. Ideally, assuming preference of the larger Fe^{2+} ions for M_4 and of Mg and Al for M_2, sodium gedrite with $X_{Mg} = \frac{1}{3}$ features $(Fe_2)^{M4}(Fe_2Mg)^{M1,M3}(MgAl)^{M2}$, showing that also

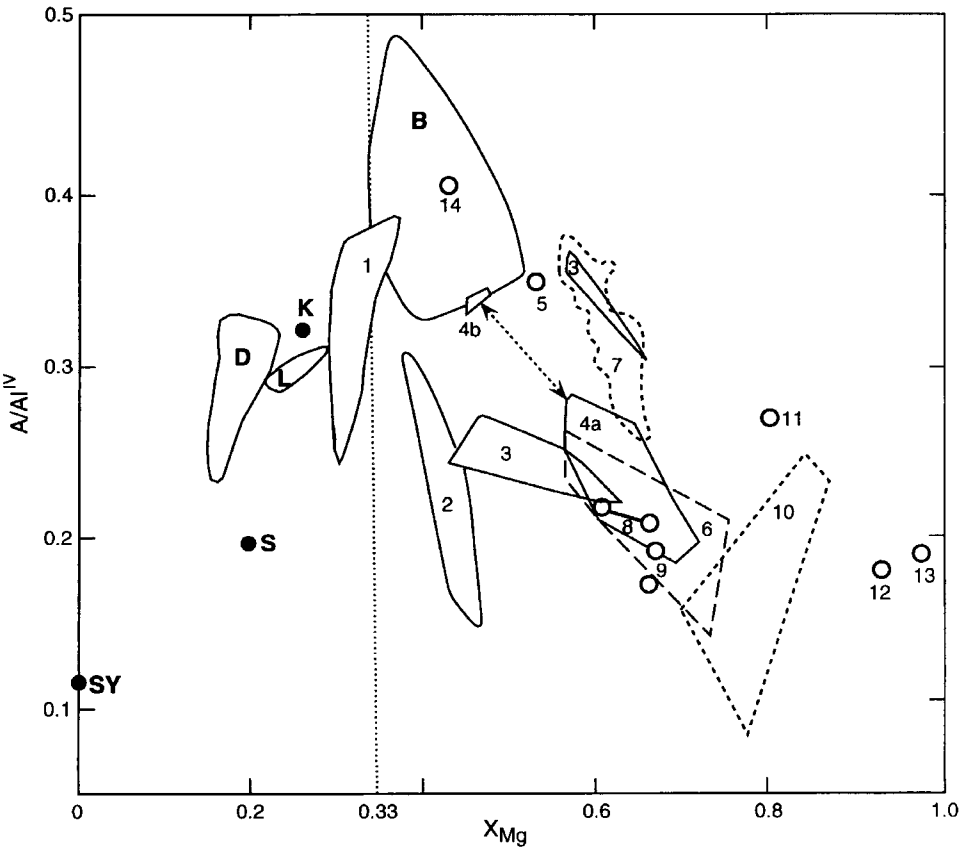

FIG. 3. Plot of Na^{A}/Al^{IV} *vs.* X_{Mg} for gedrites from various areas after Berg (1985). Data B and 1–14, after Berg (1985); S: Seitsaari (1956); SY: Seki and Yamamata (1957); K: Kroonenberg (1976); D: Damman (1988); L: this paper. Arrow bridges miscibility gap between compositions of fields 4 (Spear, 1980).

in the three M_1+M_3 sites X_{Mg} = 1/3. On these grounds, it is speculated that one factor promoting the ED substitution may be the allocation of Fe^{2+} in the two M_1 sites and Mg in the M_3 site.

Subsilicic sodium gedrites with other Fe-rich gedrites also take an aberrant position in a diagram used by Robinson *et al.* (1982) to demonstrate that $\Sigma(Al,Fe^{3+},Ti)^{M2}$ peaks at the point that the M_1+M_3 sites are filled with Mg_3. Robinson *et al.* (1982) tentatively explained their observation with the notion that the filling of the M_1 and M_3 sites with the relatively small Mg ions, thereby collapsing the structure somewhat, might promote a reduction in the mean cation size in M_2, which is accomplished by the TS substitution. Obviously, the very high to maximal TS substitutions shown by very Fe-rich gedrites are at variance with that explanation (Fig. 4). The available data suggest that TS substitution in orthoamphiboles is promoted by dominance at the M_1+M_3 sites of ions of similar size, and, dismissing Schumacher's intergrown material at the peak of the original figure, more strongly so by the larger Fe^{2+} than by the smaller Mg^{2+} ions.

Paragenesis of subsilicic sodium gedrite–biotite–(cordierite)–albite–quartz

Considering the leptite's very Ca-deprived composition and the essential alkali content of three important phases, the paragenesis is well represented in an AAlkF diagram. As shown by Fig. 5, cordierite-sekaninaite may have been a coexisting phase. Feasibly, it altered to chlorite. Growth of MgFe-amphibole or hornblende, often found associated with medium-grade gedrite (Robinson *et al.*, 1982), was prevented by the rock's high Al_2O_3/(MgO+FeO) (Fig. 5) and deficient CaO. Dearth of Ca is further reflected in the almost pure albite composition of the plagioclase (Table 2), despite the medium-grade metamorphism.

The rock's deficiency in K can be held responsible for the virtual absence of K in feldspar (0.1% Or in albite) and for the notable presence of 0.094 Na a.p.f.u in the rock's only K-phase biotite, for which 0.10 Na is an uncommon, relatively high value (Guidotti, 1984). K is not present in the amphibole, nor was it found in any of the subsilicic sodium gedrites reported so far. This is quite comprehensible, as the comparatively small (distorted octahedral) A-site, intrinsic to the *Pnma* structure (Papike and Ross, 1970), makes orthoamphiboles less suitable for allocating the large K^+ ion.

Apart from known preferences for K and Ti and for Na, Ca and Mn, respectively, biotite and subsilicic sodium gedrite show remarkably similar Si:Al:(Mg+Fe), be it with lower X_{Mg} for the amphibole (Table 3, Fig. 5). This suggests similar petrochemical roles for mica and amphibole in this rock, their relative abundances mainly modified by available K and Na.

Subsilicic sodium gedrite is closely associated with quartz in all described occurrences; equilibrium

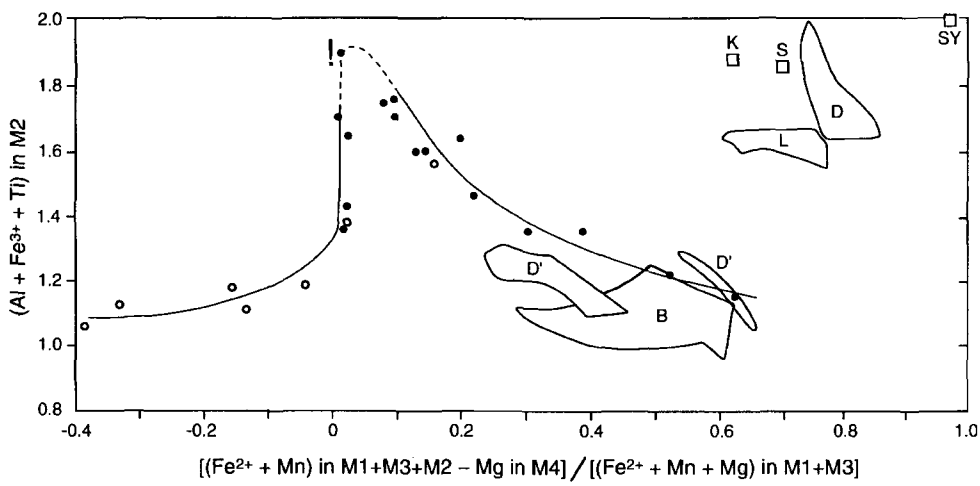

FIG. 4. Plot of Al+Fe^{3+}+Ti in M_2 *vs.* (Fe^{2+}+Mn)/(Fe^{2+}+Mn+Mg) in M_1+M_3 for orthoamphiboles coexisting with cordierite and/or staurolite, relating octahedral Al, Fe^{3+} and Ti to the distribution of Mg, Fe and Mn over the M_1, M_3 and M_4 sites. Open and filled circles and curve after Robinson *et al.* (1982); ! marks point based on Schumacher's intergrown two-phase material; B: Berg (1985); S: Seitsaari (1956); SY: Seki and Yamamata (1957); K: Kroonenberg (1976); D, D': Damman (1988, 1989); L: this study.

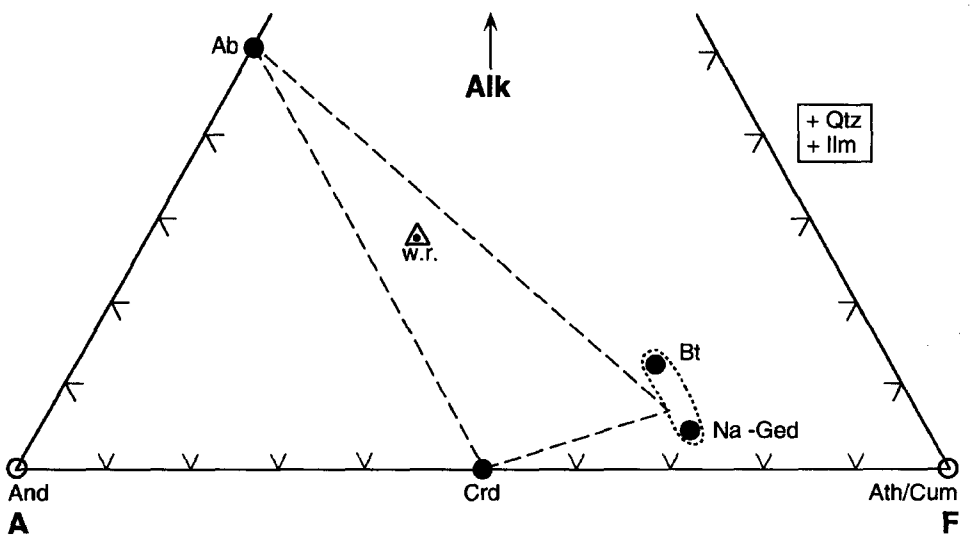

FIG. 5. AAlkF diagram projected from quartz and ilmenite. A = $Na_2O + K_2O$; A = $Al_2O_3 + 2TiO_2$; F = FeO + MnO + MgO – TiO_2; w.r. = whole rock. Note the close projections of biotite and subsilicic sodium gedrite, merely separated by different K_2O and Na_2O contents. Symbols for minerals after Kretz (1983).

growth is indicated by their symplectitic intergrowth (Kroonenberg, 1976) and by the sharp contacts of the amphibole's {210} with the annealed quartz-bearing matrix in the Nordmark leptite. Clearly, MgFe-orthoamphiboles do not concur with the suggestion (Hawthorne, 1983) that amphiboles with $Al^{IV} > 2$ occur (only) in silica-deficient environments.

Acknowledgements

We thank Frank Beunk and Wim Drucker for the XRFS whole-rock analysis and the XRD photograph, and Prof. Bernard Leake for useful, constructive remarks in his review. This is publication NSG 951110 of the Netherlands Research School of Sedimentology. Reactions to lint@geo.vu.nl (or fax +20 6462457) are welcome.

References

Baker, J.H. and De Groot, P.A. (1983) *Contrib. Mineral. Petrol.*, **82**, 119–30.

Berg, J.H. (1985) *Amer. Mineral.*, **70**, 1205–10.

Damman, A.H. (1988) *Mineral. Mag.*, **52**, 193–200.

Damman, A.H. (1989) *Amer. Mineral.*, **74**, 589–637.

Fabriës, J. and Perseil, E.A. (1971) *Bull. Soc. fr. Minéral. Cristallogr.*, **94**, 385–95.

Guidotti, C.V. (1984) *Reviews in Mineralogy*, **13**, 357–468.

Hawthorne, F.C. (1983) *Canad. Mineral.*, **21**, 173–480.

Kretz, R. (1983) *Amer. Mineral.*, **68**, 277–9.

Kroonenberg, S.B. (1976) PhD Thesis, University of Amsterdam, *Geol. Mijnb. Dienst Suriname, Mededeling*, **25**, 109–289.

Lagerblad, B. and Gorbatschev, R. (1985) *Geol. Rundsch.*, **74**, 33–49.

Leake, B.E. (1968) *Geol. Soc. Amer. Spec. Paper*, **98**, 210 pp.

Leake, B.E. (1978) *Mineral. Mag.*, **42**, 533–63.

Le Maitre, R.W. (1976) *J. Petrol.*, **17**, 573–85.

Linthout, K. (1983*a*) *Terra Cognita*, **3**, 257–8.

Linthout, K. (1983*b*) *Terra Cognita*, **3**, 179–80.

Magnusson, N.H. (1970) *S.G.U.*, **C 643**, 1–364.

Papike, J.J. and Ross, M. (1970) *Amer. Mineral.*, **55**, 1945–72.

Popp, R.K., Gilbert, M. and Craig, J.R. (1976) *Amer. Mineral.*, **61**, 1267–79.

Robinson, P., Ross, M. and Jaffe, H.W. (1971) *Amer. Mineral.*, **56**, 1005–41.

Robinson, P., Spear, F.S., Schumacher, J.C., Laird, J., Klein, C., Evans, B.W. and Doolan, B.L. (1982) *Reviews in Mineralogy*, **9B**, 1–227.

Roep, Th. and Linthout, K. (1990) *Sed. Geol.*, **61**, 239–51.

Schumacher, J.C. (1980) *Geol. Soc. Amer. Abstracts with Progr.*, **12**, 518.

Seitsaari, J. (1956), *Bull. Commission géol. Finlande*, **172**, 77–83.

Seki, Y. and Yamasaki, M. (1957) *Amer. Mineral.*, **42**, 506–20.

Spear, F.S. (1980) *Amer. Mineral.*, **65**, 1103–18.

Spear, F.S. (1993) *Metamorphic phase equilibria and*

pressure-temperature-time paths, 799 pp. Monograph M.S.A, Washington D.C.
Vallance, T.G. (1967) *J. Petrol.*, **8**, 84–96.

[*Manuscript received 18 January 1995; revised 29 March 1995*]

KEYWORDS: subsilicic sodium gedrite, quartz keratophyric protolith, Nordmark, Sweden.

MINERALOGICAL MAGAZINE, APRIL, VOL. 60, PP 387–388

Clinobisvanite, eulytite, and namibite from the Pala pegmatite district, San Diego Co., California, USA

Eugene E. Foord

MS 905, U.S. Geological Survey, Box 25046 Denver Federal Center, Denver, CO 80225, USA

THE 100 Ma complex LCT-type composite pegmatite-aplite dykes, intruded into various units of the Southern California Batholith, are known to contain bismuth minerals. Jahns and Wright (1951) reported the following primary and secondary bismuth minerals from the quartz-rich cores of a number of dykes in the Pala district, San Diego Co., California: native bismuth, bismuthinite, bismite, bismutite, and beyerite. The Little Three pegmatite-aplite dyke in the Ramona district, contains minor amounts of native bismuth, beyerite, bismite, bismutite, and pucherite (Shigley *et al.*, 1986; Foord *et al.*,1989). The Himalaya dyke system in the Mesa Grande district contains bismuth, bismutite, pucherite and beyerite. All of these minerals are sparse but characteristic of highly evolved granitic pegmatites.

Additional mineralogical studies in the Pala district indicate that at least three additional bismuth minerals not reported by Jahns and Wright (1951) or Jahns (1979) are present. The occurrence of namibite from Bohemia was recently reported by Mrázek *et al.* (1994). Namibite was reported in 1991 from the Pala district by Foord *et al.* (1991).

All minerals were identified by X-ray diffraction, SEM-EDS analyses and by electron-microprobe analyses. Fine-grained emerald-green namibite intergrown with fine-grained, tan clinobisvanite and beyerite occurs in small pod-like masses in quartz-rich 'pocket-pegmatite' in the White Queen mine on Hiriart Mountain. A total of several tens of grams of material was recovered. Electron-microprobe analyses of the clinobisvanite and namibite are given in Table 1.

An 0.5 kg mass of red-orange crystalline (individual crystals to several mm long) clinobisvanite and cream-white to tan radiating hemispheres (to several mm) of eulytite, $Bi_4(SiO_4)_3$, and associated albite occurring in quartz-rich core-zone pegmatite was found in the Elizabeth "R" mine on Chief Mountain. While eulytite is known to be cubic, and occurring in hextetrahedral crystals, the radiating and semi-globular aggregate habit agrees perfectly with that of material from both Schneeberg and

TABLE 1. Electron-microprobe analyses for clinobisvanite and namibite from the White Queen mine

	Clinobisvanite (ave. of five analyses)	Namibite (ave. of five analyses)
V_2O_5	27.0	14.1
CuO	–	12.5
Bi_2O_3	72.0	71.9
CaO	0.9**	0.1
H_2O	–	1.4*
Total	99.9	100.0

* —by difference. ** — minor beyerite contaminant.